Structural Chemistry (2020) 31:133–140
https://doi.org/10.1007/s11224-019-01385-y

ORIGINAL RESEARCH

Hydrazine trapping ability of $Si_{12}C_{12}$ fullerene-like nanoclusters: a DFT study

Rezvan Rahimi [1,2] · Mohammad Solimannejad [1,2]

Received: 16 April 2019 / Accepted: 25 June 2019 / Published online: 4 July 2019

Abstract
In this study, the nondissociative hydrazine (N_2H_4) adsorption on the surface of $Si_{12}C_{12}$ nanoclusters have been investigated using density functional theory at wB97XD/6-31G(d) computational level. It is shown that $Si_{12}C_{12}$ nanocage can hold up to five N_2H_4 molecules with the maximum average adsorption energy per hydrazine molecule of − 46.11 kcal/mol. The calculated hydrazine uptake capacity of desired nanocage reached up to 25% which are lies in the desirable range for practical applications. The results show that adsorption of hydrazine monomers on $Si_{12}C_{12}$ nanocage are more appropriate than adsorption of hydrazine dimers.

Keywords Hydrazine · $Si_{12}C_{12}$ nanocage · DFT

Introduction

The hydrazine molecule is an important compound that included amine with a desirable hydrogen amount of 12.5 wt% [1, 2]. This molecule extensively applied in the military technologies and chemical industry for several applications as hydrogen storage [3], rocket fuel for satellite emission [4], fuel cell [5, 6], missile system [7], and strong reducing agent [8].

The N_2H_4 molecule is a hyper-toxic moiety with carcinogenicity which leads to skin and lung cancers. Unfortunately, by inhalation of hydrazine, the function of entire body, especially nervous and respiratory system is likely to seriously damaged. So it is urgent to diagnosis and finds an ideal material in order to detecting, prohibition, and decomposition harmful substances similar hydrazine molecules in surrounding environments. So far, lot of studies have been done on this issue [9].

Structure of hydrazine has been determined experimentally by Kohata et al. [10], using electron diffraction method. In the ab initio study by Cabaleiro-Lago and Ríos interactions in hydrazine clusters of one to four molecules have been reported [11]. It is demonstrated that hydrazine monomer (N_2H_4) and dimer $(N_2H_4)_2$ molecules are composed of two stable conformations and one saddle point, respectively. Moreover, the equilibrium structure, the dipole moment and the two rotation barrier heights for hydrazine has been proposed by Dyczmons [12].

So far, the adsorption and dissociation of hydrazine molecule on the surface of various metal or alloy systems like Ir [13], Ni [14, 15], Fe [16], Rh [17], and Ni–M (M = Fe, Pt, Ir, Pd, and Rh) [18, 19] have been studied theoretically. Adsorption and decomposition of N_2H_4 molecule on the perfect and defective copper surfaces via DFT calculations have been reported by Tafreshi and coworkers [20]. Kinetics and mechanisms of hydrazine decomposition in the presence of catalytic materials have been proposed [21–24]. Recently, catalytic dehydrogenation of hydrazine on silicon-carbide nanotubes has been reported [25].

In the past few years, silicon carbide (SiC) has drawn lots of attention because of it as one of the best biocompatible materials used in biophotonics, bioimaging, and diagnostics. On the other hand, these materials in contemporary investigations frequently studied due to unique physicochemical properties of such as high-power, high frequency, high-temperature semiconductors, wide band gap and high thermal conductivity [26–28]. Lately, the synthesis of SiC different nanostructures including nanowires [29, 30], nanotubes [31, 32], nanorods [33, 34], hollow

✉ Mohammad Solimannejad
m-solimannejad@araku.ac.ir

[1] Department of Chemistry, Faculty of Sciences, Arak University, Arak 38156-8-8349, Iran

[2] Institute of Nanosciences and Nanotechnology, Arak University, Arak 38156-8-8349, Iran

nanospheres [35], nanocages [36], and tetrapods [37] have been reported. According to recent theoretical studies, geometries and stability of $Si_{12}C_{12}$ isomers have been already studied, and $Si_{12}C_{12}$ nanocage appears to be more stable than other isomers [26].

Recently, nonlinear optical (NLO) response of $Si_{12}C_{12}$ nanocage decorated with alkali metals (M = Li, Na, and K) [38] and sensing performance of $Si_{12}C_{12}$ nanocage toward toxic cyanogen gas [39] have been reported by our research group. In continue, to find out different applications of $Si_{12}C_{12}$ nanocage, capability of this nanocage for removal of hydrazine from environmental systems is considered. The results of present study may open new doors in application of silicon-carbide nanoclusters in industry and technology.

Computational details

Geometry optimizations have been performed using the density functional theory (DFT) at the wB97XD/6-31G(d) level [40]. It is noteworthy that one of long-range corrected hybrid density functional with improve dispersion corrections is wB97XD functional that used to calculate empirical dispersion energy correction. Many reports proved accuracy of wB97XD functional for thermodynamic and kinetic calculations as well as non-covalent interactions than other methods [41]. The natures of the stationary points have been investigated via frequency analysis at the same computational level. All calculations were performed utilizing Gaussian 09 code [42].

In this study, the HOMO–LUMO gap (HLG) is determined using Eq. (1), where ε_H and ε_L are the highest occupied molecular orbital energy (HOMO) and lowest unoccupied molecular orbital energy (LUMO), respectively.

$$HLG = \varepsilon_L - \varepsilon_H \quad (1)$$

The average adsorption energy (E_{ads}) per hydrazine molecule has been obtained through Eq. (2).

$$E_{ads} = \left(E_{complex} - E_{Si12C12} - nE_{N2H4} \right)/n \quad (2)$$

Where $E_{complex}$ is total energy of the studied complexes, $E_{Si12C12}$ is total energy of $Si_{12}C_{12}$ nanocage and nE_{N2H4} is the total energy of hydrazine molecules respectively. The n is number of adsorbed hydrazine molecules.

Results and discussion

Geometric and electronic property of $Si_{12}C_{12}$ nanocage

Optimization of $Si_{12}C_{12}$ nanocage is performed at wB97XD/6-31G(d) computational level. The desired $Si_{12}C_{12}$ nanocage consists of six tetragonal and eight hexagonal rings. Two individual Si–C bonds are distinguishable in the $Si_{12}C_{12}$ nanocage, one is shared between two hexagons (b66) with length about 1.77 Å, and the other is shared between a tetragon and a hexagon (b64) with length of 1.82 Å (see Fig. 1). It seems that the participation of p orbital is increased for (b64) bonds in comparison to (b66). Therefore, the bond lengths of (b64) are larger than (b66). Frontier molecular orbital energies (HOMO and LUMO) and the energy difference between HOMO and LUMO (HLG) of considered nanocage are − 8.04, − 1.02, and 7.02 (eV) respectively.

Adsorption and decomposition of hydrazine over surface of $Si_{12}C_{12}$ nanocage

To find the ability to decompose hydrazine by $Si_{12}C_{12}$ nanocage, different situations for the approach of a hydrazine molecule to the surface of $Si_{12}C_{12}$ nanocage are considered, including; on top of a Si and C atoms, over hexagonal and square rings, and on the top of a b66 or a b64 bond. After full optimization of desired systems, one structure with no imaginary vibrational frequencies was established for N_2H_4…$Si_{12}C_{12}$ complexes. This structure is based on strong interaction between lone pair of nitrogen of hydrazine with Si atom of nanocage (**I**) with adsorption energy of − 45.30 kcal/mol. The distance between nitrogen atom in hydrazine and silicon atom in $Si_{12}C_{12}$ nanocage is 1.96 Å in this complex. During the formation of this complex the hybridization of the interacting silicon atom changes from sp^2 to sp^3. On the other hand, elongation of N–N bond of hydrazine is reported due to chemisorption of hydrazine over surface of nanocage.

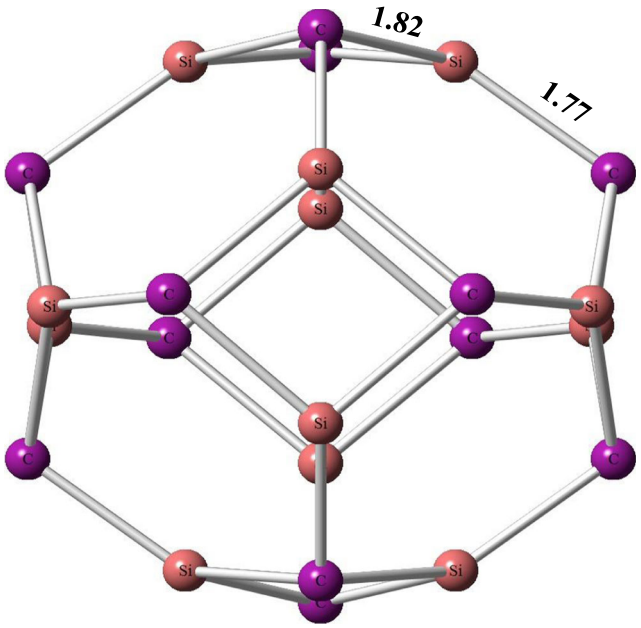

Fig. 1 Optimized geometry of the pristine $Si_{12}C_{12}$

The energy profiles for the reaction pathways of N_2H_4 dissociation over surface of $Si_{12}C_{12}$ has been shown in Fig. 2. The values of activation energies (E_{act}), imaginary frequencies (ν), and thermodynamic parameters of the considered reactions have been computed and listed in Table 1. The reaction begins with the interaction of hydrazine with the surface of nanocage and leads to the formation of an intermediate **I**. The reaction path **R1** begins with the dissociation of N–H bond of N_2H_4 via **TS-1.** Afterward, the resulting hydrogen atom from cleavage of N–H bond is transferred to the top site of C atom of surface to form **P1**. The activation barrier for formation of **P1** is 24.28 kcal/mol (Fig. 2). An imaginary frequency of 1730i cm^{-1} is confirmed by vibrational frequency calculation for **TS-1**. Formation of **P1** is an exothermic reaction and spontaneous process at room temperature with enthalpy change (ΔH_{298}) of − 19.75 kcal/mol and ΔG_{298} value of − 20.07 kcal/mol. In the next step, the chemically bonded N_2H_3 group may continue reaction with transfer of another hydrogen on other C atom of nanocage. At the same time, the bond between Si of nanocage and N_2H_2 is cracked that lead to formation of **P2.** The corresponding transition state

Table 1 Calculated BSSE corrected activation energies, imaginary frequencies, change of Gibbs free energy (ΔG_{298}), and change of enthalpy (ΔH_{298}) for decomposition of N_2H_4 over surface of $Si_{12}C_{12}$

Reaction pathway	E_{act} (kcal/mol)	ν (cm^{-1})	ΔG_{298} (kcal/mol)	ΔH_{298} (kcal/mol)
Pathway *R*1				
I → P1	24.28	1730i	− 20.07	− 19.75
P1 → P2	47.84	1570i	13.32	10.86
P2 → P3	52.68	1470i	3.32	6.22
P3 → P4	7.33	1178i	− 52.36	− 48.51
Pathway R2				
I → P5	74.69	765i	− 32.15	− 31.92

TS-2 and **P2** are depicted in Fig. 2. The energy-barrier height of this step is 47.84 kcal/mol with an imaginary frequency of 1570i cm^{-1}. Process of product formation of **P2** is an endothermic reaction with enthalpy change (ΔH_{298}) of 10.86 kcal/mol and ΔG_{298} value of 13.32 kcal/mol. The reaction continues with chemical bonding of N_2H_2 with surface of nanocage concurrent with the transition of one hydrogen of

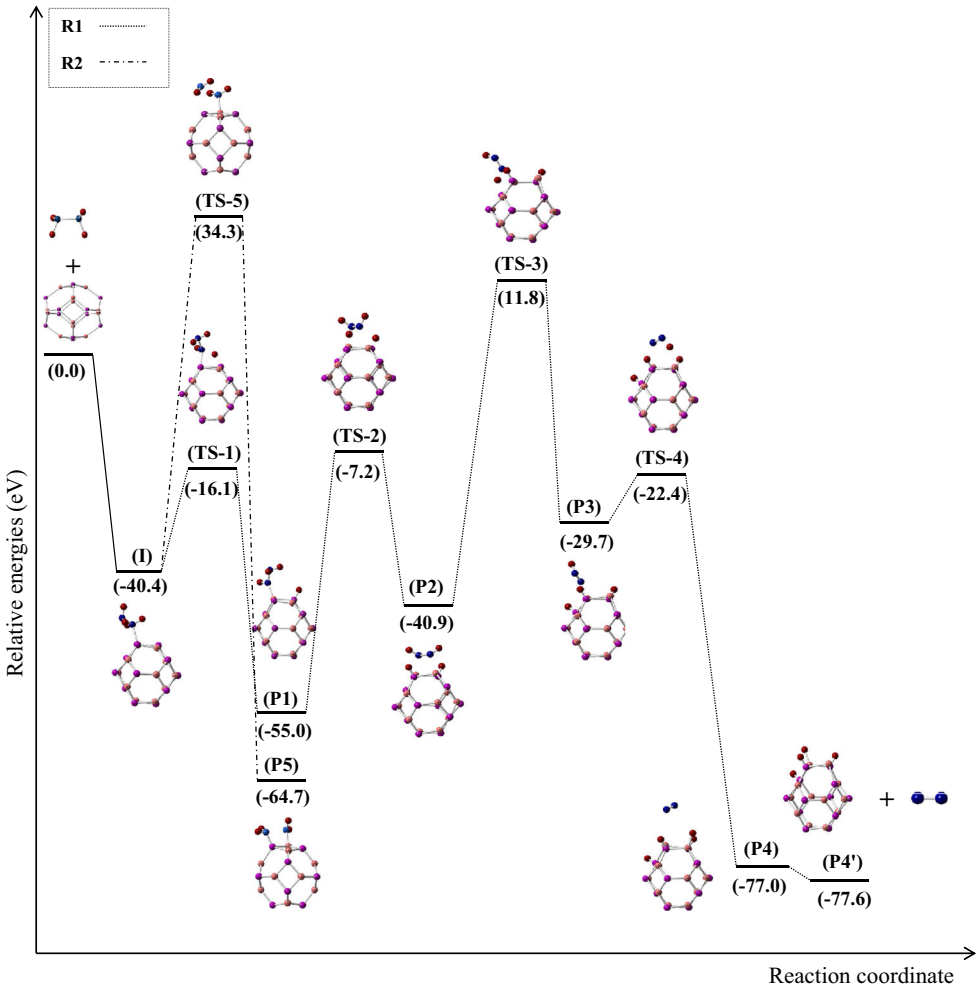

Fig. 2 Reaction pathways of N_2H_4 decomposition on the surface of $Si_{12}C_{12}$ nanocage

N_2H_2 to another C atom of nanocage to form **P3.** The reaction barrier for becoming **P2** to **P3** is about 52.68 kcal/mol (Table 1) with the imaginary frequency of 1470i cm^{-1} for **TS-3** transition state. Reaction of product formation of **P3** is endothermic with enthalpy change of 6.22 kcal/mol and ΔG_{298} value of 3.32 kcal/mol. Follow the path of reaction, **P4** is obtained through transfer of hydrogen of chemically bonded N_2H group to Si atom of surface synchronous with release of N_2 from surface of nanocage. **P4** is obtained through pass of system from **TS-4** with an imaginary frequency of 1178i cm^{-1}. The values of activation energies, ΔH_{298}, and ΔG_{298} for the path of conversion of **P3** to **P4** are 7.33 kcal/mol, − 48.51 kcal/mol, and − 52.36 kcal/mol respectively.

In the other possible path of reaction **R2**, the N–N bond of hydrazine is activated for breaking over surface of nanocage to form **P5** as depicted in Fig. 2. The transition state **TS-5** is confirmed by the attendance of an imaginary frequency of 765i cm^{-1} corresponding to the N–N stretching vibration mode on the surface of nanocage. The formation of **P5** is feasible if the system can overcome the relatively high energy barrier of 74.69 kcal/mol. This process is exothermic by − 31.92 kcal/mol due to stability of two newly formed NH_2 groups on the nanocage surface.

The calculated activation energy required for initial step of hydrazine dissociation over the surface of $Si_{12}C_{12}$ nanocage is large for both reaction paths **R1** (24.28 kcal/mol) and **R2** (74.69 kcal/mol). It is shown that CO oxidation with a reaction barrier of less than 11.53 kcal/mol is expected to occur at room temperature [43]. So it is concluded that adsorption of hydrazine over $Si_{12}C_{12}$ nanocage is not dissociative at room temperature.

Uptake of hydrazine molecules by $Si_{12}C_{12}$ nanocage

It has been concluded from above discussion that hydrazine molecule is not decomposed over the surface of $Si_{12}C_{12}$ readily. So in continuation of our study, the capability of $Si_{12}C_{12}$ nanoclusters toward uptake of hydrazine molecules is investigated. It has been mentioned before that structure **I** is local minimum on the potential energy surface of $Si_{12}C_{12}…N_2H_4$ complexes. Electronic properties of this considered complex has been analyzed with calculation of HOMO, LUMO and HOMO–LUMO gap energies which are − 7.53, − 0.51, and 7.02 eV respectively (Table 2).

To figure out potency of desired nanocage for interaction with more hydrazine molecules, more than one hydrazine molecules are approached over surface of $Si_{12}C_{12}$. N_2H_4 molecule was added one by one to find out the maximal adsorption capacity. It is seen that $Si_{12}C_{12}$ nanocage can hold up to five N_2H_4 molecules with average adsorption energy with the maximum average adsorption energy per hydrazine molecule in the range from − 41.94 to − 46.11 kcal/mol. When the sixth N_2H_4 molecule was attached, the imaginary frequency for the optimized structure shows that adsorption of sixth N_2H_4 molecule is not feasible. The local minimum structures for $2N_2H_4$ (**II**), $3N_2H_4$ (**III**), $4N_2H_4$ (**IV**), and $5N_2H_4$ (**V**) complexes with nanocage at wB97XD/6-31G (d) computational level are depicted in Fig. 3. The values of adsorption energies E_{ads}, HOMO, and LUMO energies with HOMO–LUMO gap (HLG) of the considered complexes have been computed and listed in Table 2. It is obvious that there is no significant change in the electronic properties of $Si_{12}C_{12}$ nanocage due to interaction with hydrazine molecules. The values of adsorption energy per number of hydrazine molecules follow the sequence **III** > **II** > **I** > **IV** > **V**.

It is obvious that the interaction of N_2H_4 molecule with the surface of $Si_{12}C_{12}$ nanocage leads to increase of HLG values in some of the complexes. However, changes in electronic property of $Si_{12}C_{12}$ nanocage due to adsorption of N_2H_4 molecules is not remarkable.

In the next step of the study, the interaction between hydrazine dimers $(N_2H_4)_2$ and $Si_{12}C_{12}$ nanocage were explored at wB97XD/6-31G (d) computational level. For this aim, most stable conformer of hydrazine dimers $(N_2H_4)_2$ [11] was approached to nanocage via interaction between lone pair of N and Si atom of nanocage (complex **VI**). Interactions of two dimers of hydrazine are also investigated and optimized geometries are presented in Fig. 3 (**VII**). The magnitude of HOMO, LUMO, and HOMO-LUMO gap (HLG) for the mentioned structures are calculated and summarized in Table 2. The HOMO-LUMO gap (HLG) values of structures **VI** and **VII** are 7.03 (eV) and 7.04 (eV) respectively.

Adsorption energies and electronic properties of studied complexes have been calculated with 6–31 + G(d) basis set including diffuse function (Table 2). Comparison of results for 6-31G(d) and 6–31 + G(d) basis set shows that adsorption energy and HLG calculated with latter is lower than former. In sum, the difference of results from these two basis sets is not remarkable.

The values of average adsorption energy per number of hydrazine for mentioned structures adherence to the following trend: **VII** > **VI**. Comparison of E_{ads} values for cluster **II** with cluster **VI** and cluster **IV** with cluster **VII** in Table 2, confirms that adsorption of hydrazine in form of monomer on the desired system are stronger than hydrazine dimers.

Moreover, the hydrazine uptake capacity of nanocage was calculated by the following equation:

$$N_2H_4(Wt\%) = \left(\frac{M_{N2H4}}{M_{N2H4} + M_{Si12C12}}\right) \times 100 \quad (3)$$

Where M_{N2H4} indicates the mass of adsorbed total number of hydrazine molecules and $M_{Si12C12}$ represents the mass of desired nanocage in this study. The calculated hydrazine uptake capacity reached up to 25% (Table 2) which are lies in the desirable range for practical applications.

Table 2 Average adsorption energies (E_{ads}), hydrazine uptake capacity of nanocage (wt%), HOMO and LUMO energies values, and HOMO–LUMO gap (HLG) for $Si_{12}C_{12}$ nanocage and considered complexes with 6-31G(d) and 6–31 + G(d) (in parenthesis) basis sets

Clusters	E_{ads} (kcal/mol)	wt%	HOMO (eV)	LUMO (eV)	HLG (eV)
I	− 45.30 (− 42.78)	6.25	− 7.53 (− 7.61)	− 0.51 (− 0.62)	7.02 (6.99)
II	− 45.45 (− 42.68)	11.76	− 7.16 (− 7.26)	− 0.10 (− 0.24)	7.06 (7.02)
III	− 46.11 (− 43.08)	16.67	− 6.85 (− 6.99)	0.44 (0.16)	7.30 (7.15)
IV	− 43.61 (− 40.88)	21.05	− 6.50 (− 6.67)	0.83 (0.47)	7.34 (7.15)
V	− 41.94 (− 39.40)	25.00	− 6.12 (− 6.31)	1.21 (0.69)	7.33 (7.01)
VI	− 33.76 (− 30.86)	11.76	− 7.42 (− 7.54)	− 0.39 (− 0.54)	7.03 (6.99)
VII	− 32.76 (− 30.08)	21.05	− 6.87 (− 7.06)	0.16 (− 0.06)	7.04 (7.00)

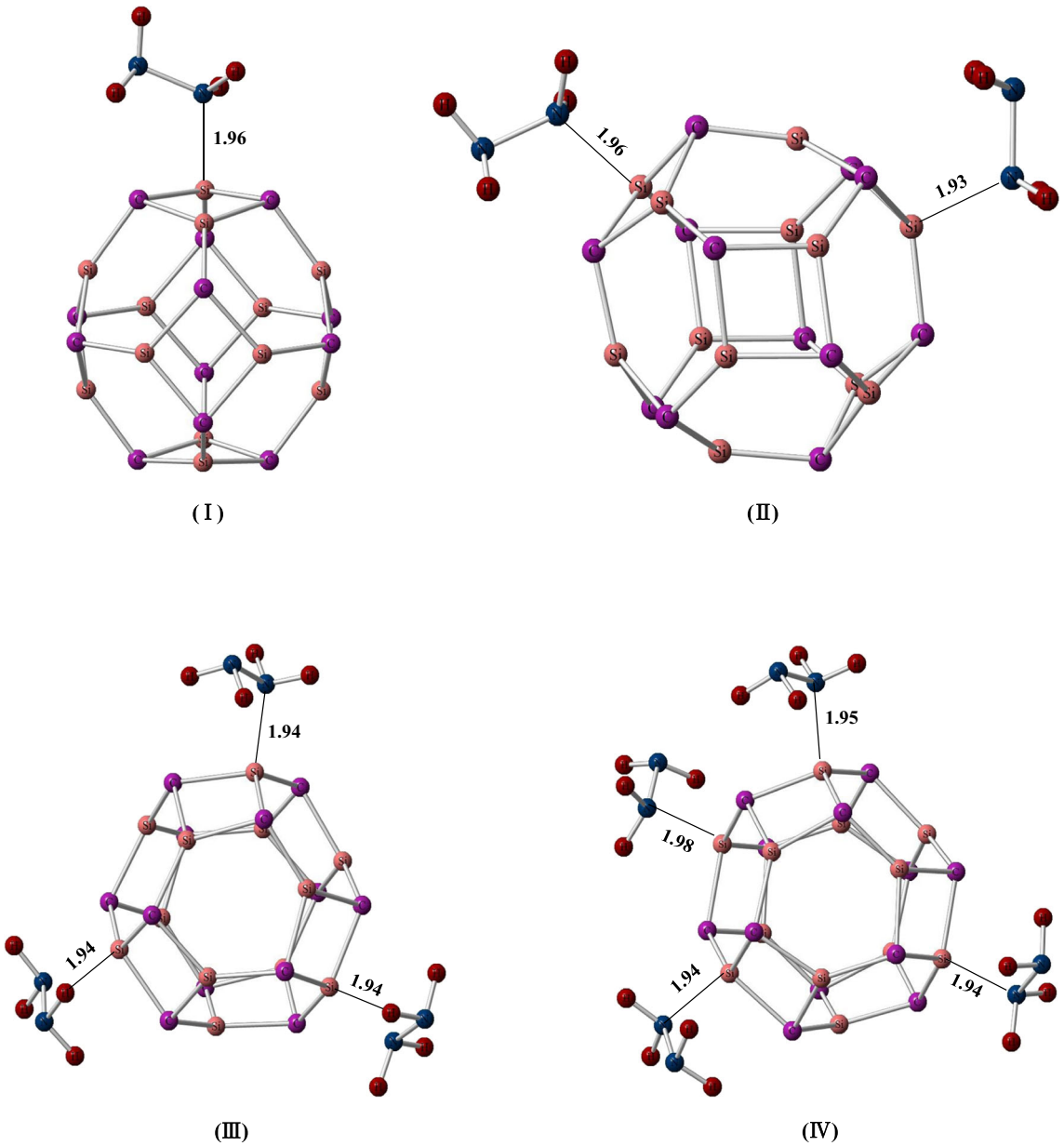

Fig. 3 Optimized geometry for the adsorption (**I**) N_2H_4, (**II**) $2(N_2H_4)$, (**III**) $3(N_2H_4)$, (**IV**) $4(N_2H_4)$, (**V**) $5(N_2H_4)$, (**VI**) $(N_2H_4)_2$, and (**VII**) $2(N_2H_4)_2$ on $Si_{12}C_{12}$ nanocage

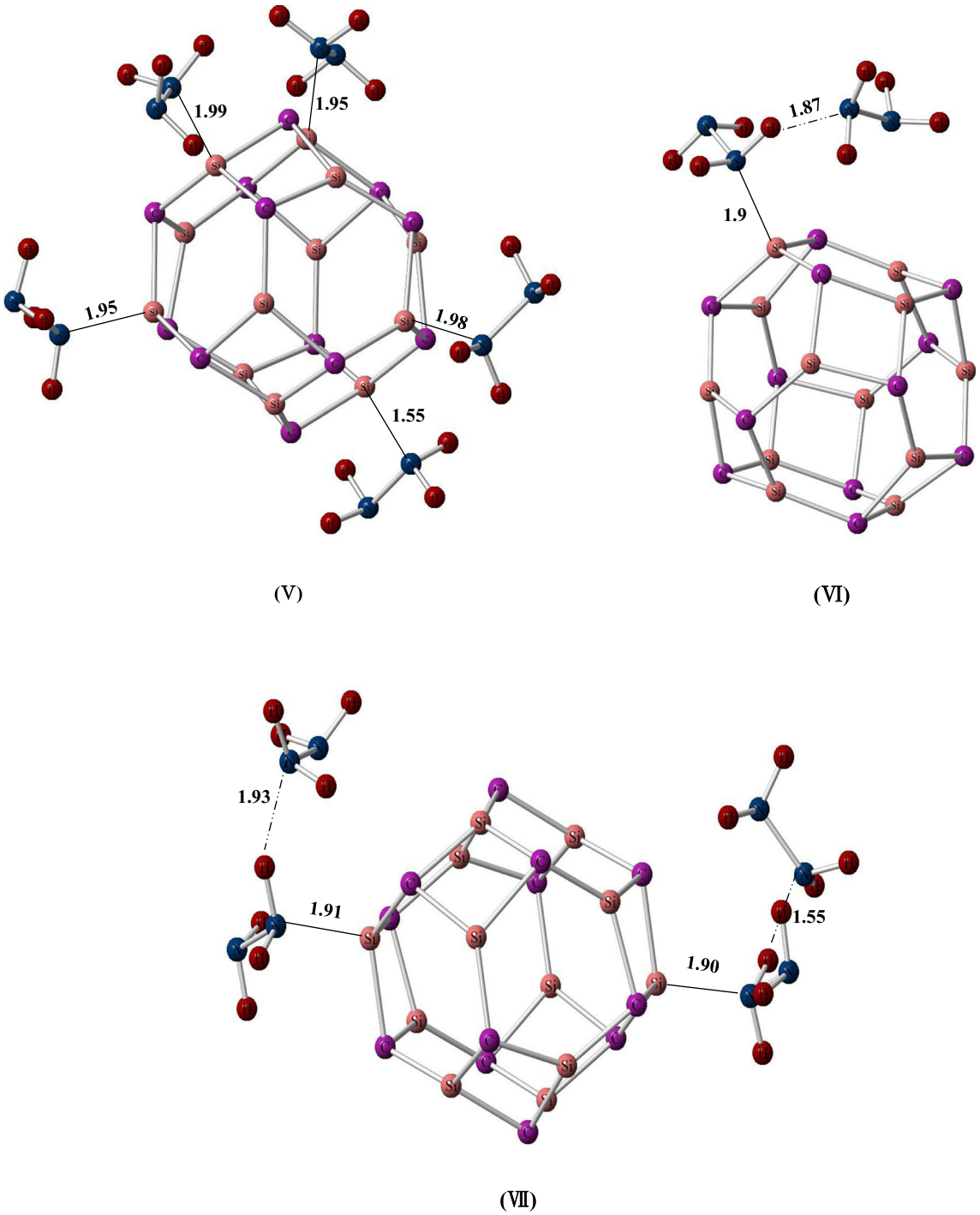

Fig. 3 (continued)

Conclusions

In this study, we have applied DFT calculations to investigate the interaction of the hydrazine monomer (N_2H_4) and dimers $(N_2H_4)_2$ with $Si_{12}C_{12}$ nanocage. Indeed hydrazine could be adsorbed over the Si atom of $Si_{12}C_{12}$ nanocage through interaction of nitrogen atom of hydrazine with Si atom of nanocage. The results of calculations show that $Si_{12}C_{12}$ nanocage could absorb up to five monomers or two dimers of hydrazine. Comparison of results confirms that adsorption

of hydrazine as monomer are more appropriate than corresponding dimers. To sum up, adsorption of hydrazine over $Si_{12}C_{12}$ nanocage is not dissociative at normal temperature, and it may be used as potential candidate for removal of hydrazine from environmental systems.

Compliance with ethical standards

Conflict of interest The authors declare that they have no conflict of interest.

References

1. Tafreshi SS, Roldan A, de Leeuw NH (2015) Density functional theory calculations of the hydrazine decomposition mechanism on the planar and stepped cu (111) surfaces. Phys Chem Chem Phys 17:21533–21546
2. Li S, Qu K, Zhao H, Ding L, Du L (2016) Clustering of amines and hydrazines in atmospheric nucleation. Chem Phys 472:198–207
3. Zhong Y-J, Dai H-B, Zhu M, Wang P (2016) Catalytic decomposition of hydrous hydrazine over NiPt/La2O3 catalyst: a high-performance hydrogen storage system. Int J Hydrog Energy 41: 11042–11049
4. Tafreshi SS, Roldan A, Dzade NY, de Leeuw NH (2014) Adsorption of hydrazine on the perfect and defective copper (111) surface: a dispersion-corrected DFT study. Surf Sci 622:1–8
5. Song J, Ran R, Shao Z (2010) Hydrazine as efficient fuel for low-temperature SOFC through ex-situ catalytic decomposition with high selectivity toward hydrogen. Int J Hydrog Energy 35:7919–7924
6. Yamada K, Asazawa K, Yasuda K, Ioroi T, Tanaka H, Miyazaki Y, Kobayashi T (2003) Investigation of PEM type direct hydrazine fuel cell. J Power Sources 115:236–242
7. Baei MT, Soltani A, Hashemian S (2016) Adsorption properties of hydrazine on pristine and Si-doped Al12N12 nano-cage. Phosphorus Sulfur Silicon Relat Elem 191:702–708
8. Ensafi AA, Mirmomtaz E (2005) Electrocatalytic oxidation of hydrazine with pyrogallol red as a mediator on glassy carbon electrode. J Electroanal Chem 583:176–183
9. Courthéoux L, Amariei D, Rossignol S, Kappenstein C (2005) Facile catalytic decomposition at low temperature of energetic ionic liquid as hydrazine substitute. Eur J Inorg Chem 2005:2293–2295
10. Kohata K, Fukuyama T, Kuchitsu K (1982) Molecular structure of hydrazine as studied by gas electron diffraction. J Phys Chem 86: 602–606
11. Cabaleiro-Lago EM, Ríos MA (1999) Ab initio study of interactions in hydrazine clusters of one to four molecules: cooperativity in the interaction. J Phys Chem A 103:6468–6474
12. Dyczmons V (2000) Six structures of the hydrazine dimer. J Phys Chem A 104:8263–8269
13. Zhang P-X, Wang Y-G, Huang Y-Q, Zhang T, Wu G-S, Li J (2011) Density functional theory investigations on the catalytic mechanisms of hydrazine decompositions on Ir (1 1 1). Catal Today 165:80–88
14. Agusta MK, David M, Nakanishi H, Kasai H (2010) Hydrazine (N2H4) adsorption on Ni (1 0 0)–density functional theory investigation. Surf Sci 604:245–251
15. Agusta MK, Kasai H (2012) First principles investigations of hydrazine adsorption conformations on Ni (111) surface. Surf Sci 606: 766–771
16. Fathurrahman F, Kasai H (2015) Density functional study of hydrazine adsorption and its NN bond cleaving on Fe (110) surface. Surf Sci 639:25–31
17. He YB, Jia JF, Wu HS (2015) The interaction of hydrazine with an Rh (1 1 1) surface as a model for adsorption to rhodium nanoparticles: a dispersion-corrected DFT study. Appl Surf Sci 327:462–469
18. He Y-B, Jia J-F, Wu H-S (2015) First-principles investigation of the molecular adsorption and dissociation of hydrazine on Ni–Fe alloy surfaces. J Phys Chem C 119:8763–8774
19. He Y-B, Jia J-F, Wu H-S (2015) Selectivity of Ni-based surface alloys toward hydrazine adsorption: a DFT study with van der Waals interactions. Appl Surf Sci 339:36–45
20. Tafreshi SS, Roldan A, de Leeuw NH (2014) Density functional theory study of the adsorption of hydrazine on the perfect and defective copper (100),(110), and (111) surfaces. J Phys Chem C 118:26103–26114
21. Zhao B, Song J, Ran R, Shao Z (2012) Catalytic decomposition of hydrous hydrazine to hydrogen over oxide catalysts at ambient conditions for PEMFCs. Int J Hydrog Energy 37:1133–1139
22. Singh SK, Xu Q (2009) Complete conversion of hydrous hydrazine to hydrogen at room temperature for chemical hydrogen storage. J Am Chem Soc 131:18032–18033
23. Gu H, Ran R, Zhou W, Shao Z, Jin W, Xu N, Ahn J (2008) Solid-oxide fuel cell operated on in situ catalytic decomposition products of liquid hydrazine. J Power Sources 177:323–329
24. Lin Y, Ran R, Guo Y, Zhou W, Cai R, Wang J, Shao Z (2010) Proton-conducting fuel cells operating on hydrogen, ammonia and hydrazine at intermediate temperatures. Int J Hydrog Energy 35: 2637–2642
25. Esrafili MD, Teymurian VM, Nurazar R (2015) Catalytic dehydrogenation of hydrazine on silicon-carbide nanotubes: a DFT study on the kinetic issue. Surf Sci 632:118–125
26. Duan XF, Burggraf LW (2015) Theoretical investigation of stabilities and optical properties of Si12C12 clusters. J Chem Phys 142: 034303
27. Mo Y, Shajahan M, Lee Y, Hahn Y, Nahm K (2004) Structural transformation of carbon nanotubes to silicon carbide nanorods or microcrystals by the reaction with different silicon sources in rf induced CVD reactor. Synth Met 140:309–315
28. Pan Z, Lai HL, Au FC, Duan X, Zhou W, Shi W, Wang N, Lee CS, Wong NB, Lee ST (2000) Oriented silicon carbide nanowires: synthesis and field emission properties. Adv Mater 12:1186–1190
29. Khataee A, Hasanzadeh A, Iranifam M, Joo SW (2015) A novel flow-injection chemiluminescence method for determination of baclofen using l-cysteine capped CdS quantum dots. Sensors Actuators B Chem 215:272–282
30. Guzelturk B, Kelestemur Y, Gungor K, Yeltik A, Akgul MZ, Wang Y, Chen R, Dang C, Sun H, Demir HV (2015) Stable and low-threshold optical gain in CdSe/CdS quantum dots: an all-colloidal frequency up-converted laser. Adv Mater 27:2741–2746
31. Keller N, Pham-Huu C, Ehret G, Keller V, Ledoux MJ (2003) Synthesis and characterisation of medium surface area silicon carbide nanotubes. Carbon 41:2131–2139
32. Taguchi T, Igawa N, Yamamoto H, Jitsukawa S (2005) Synthesis of silicon carbide nanotubes. J Am Ceram Soc 88:459–461
33. Tang C, Fan S, Dang H, Zhao J, Zhang C, Li P, Gu Q (2000) Growth of SiC nanorods prepared by carbon nanotubes-confined reaction. J Cryst Growth 210:595–599
34. Khan A, Jacob C (2014) Random and self-aligned growth of 3C-SiC nanorods via VLS–VS mechanism on the same silicon substrate. Mater Lett 135:103–106
35. Li P, Xu L, Qian Y (2008) Selective synthesis of 3C-SiC hollow nanospheres and nanowires. Cryst Growth Des 8:2431–2436
36. Zhao M, Xia Y, Mei L (2012) Silicon carbide Nanocages and nanotubes: analogs of carbon fullerenes and nanotubes or not? J Comput Theor Nanosci 9:1999–2007

37. Magyar AP, Aharonovich I, Baram M, Hu EL (2013) Photoluminescent SiC tetrapods. Nano Lett 13:1210–1215
38. Solimannejad M, Rahimi R, Kamalinahad S (2017) Nonlinear optical (NLO) response of Si12C12 Nanocage decorated with alkali metals (M= Li, Na and K): a theoretical study. J Inorg Organomet Polym Mater 27:1234–1242
39. Solimannejad M, Anjiraki AK, Kamalinahad S (2017) Sensing performance of cu-decorated Si12C12 nanocage towards toxic cyanogen gas: a DFT study. Mater Res Express 4:045011
40. Frisch MJ, Pople JA, Binkley JS (1984) Self-consistent molecular orbital methods 25. Supplementary functions for Gaussian basis sets. J Chem Phys 80:3265–3269
41. Chai J-D, Head-Gordon M (2008) Long-range corrected hybrid density functionals with damped atom–atom dispersion corrections. Phys Chem Chem Phys 10:6615–6620
42. Frisch M, Trucks G, Schlegel H B, Scuseria G, Robb M, Cheeseman J, Scalmani G, Barone V, Mennucci B, Petersson G (2009) Gaussian 09, revision a. 02, gaussian Inc., Wallingford, CT 200
43. Lu YH, Zhou M, Zhang C, Feng YP (2009) Metal-embedded graphene: a possible catalyst with high activity. J Phys Chem C 47:20156–20160